Article

Discovery Medicine 2026; 38(210): 2210–2219
https://doi.org/10.24976/Discov.Med.202638210.173

Silencing of Voltage-Dependent Anion Channel 2 Alleviates Myocardial Ischemia-Reperfusion Injury by Reversing Autophagy-Induced Ferroptosis of Cardiomyocytes

Hantao Jiang[1,†], Ying Jin[1,†], Chao Feng[1], Bei Ren[1], Jing Zhang[1], An Yan[1], Jinping Feng[1,*]

[1]Department of CICU, Tianjin Chest Hospital (Heping Campus), 300051 Tianjin, China
*Correspondence: fengjianping_FJp@163.com (Jinping Feng)
[†]These authors contributed equally.
Submitted: 9 February 2026 Revised: 11 March 2026 Accepted: 20 May 2026 Published: 23 July 2026

Background: Myocardial ischemia-reperfusion injury (IRI) is a critical pathological process impacting clinical outcomes after cardiac events. While the voltage-dependent anion channel 1 (VDAC1) has been implicated in IRI progression, the role of its isoform, VDAC2, remains less defined. Herein, we investigated the specific role and potential mechanism of VDAC2 in myocardial IRI.

Methods: H9c2 cardiomyocytes of rats were transfected and underwent hypoxia/reoxygenation (H/R) modeling, after which treatment with Rapamycin was performed. Key molecules, including VDAC2, autophagy-related proteins, and mechanistic target of rapamycin complex 1 (mTORC1) signaling components, were quantified using quantitative real-time PCR and Western Blotting. Cell viability and apoptosis were assessed via Cell Counting Kit-8 assay and flow cytometry. Creatine kinase (CK) and lactate dehydrogenase (LDH) activities, along with Fe^{2+} content, were measured to evaluate myocardial injury and ferroptosis.

Results: VDAC2 expression was promoted in H/R-induced H9c2 cells. VDAC2 silencing promoted viability and suppressed apoptosis of H/R-induced H9c2 cells. VDAC2 silencing reversed H/R-induced down-regulation of mTORC1 signaling (p-mTOR/mTOR and p-p70s6k/p70s6k ratios), and up-regulation of CK and LDH activities, Fe^{2+} content, and autophagy markers (Beclin-1 and LC3B-II/LC3B-I ratio) in H9c2 cells. However, Rapamycin reversed the protective effect of VDAC2 silencing on H/R-induced H9c2 cells, as evidenced by enhanced autophagy and apoptosis, elevated Fe^{2+} levels, and decreased viability.

Conclusion: VDAC2 silencing alleviates myocardial IRI potentially through modulation of autophagy and ferroptosis-related processes of cardiomyocytes. These findings identify a novel role of VDAC2 in IRI pathogenesis and position it as a promising candidate for therapeutic intervention in cardiac reperfusion injury.

Keywords: VDAC2; ferroptosis; ischemia reperfusion; mTORC1 signaling pathway; autophagy

Introduction

Ischemic heart disease (IHD) is a life-threatening condition globally [1], the most severe manifestation of which is acute myocardial infarction, imposing substantial burdens on both society and individuals [2,3]. The coronary artery perfusion thrombolysis remains the primary, effective treatment regimen for acute myocardial infarction [4]. However, this therapeutic intervention paradoxically initiates myocardial ischemia-reperfusion injury (IRI), a complication with an increasing morbidity rate [5]. Increased autophagy has been reported to be a hallmark of IRI [6,7]. Given the high incidence of IRI and the limited efficacy of current treatment methods, exploring novel anti-IRI interventions is of great significance.

MiR-183-5p has been confirmed to attenuate myocardial IRI via down-regulating Voltage Dependent Anion-selective Channel 1 (VDAC1) in mice [8]. As one of the channels in mitochondria and another isoform of the VDAC family, VDAC2 has emerged as a critical regulator of cardiac physiology and pathology. Accumulating evidence highlights the pivotal role of VDAC2 in maintaining cardiac homeostasis; VDAC2 is implicated in cardiac local Ca^{2+} signaling via facilitating mitochondrial Ca^{2+} uptake and restricting Ca^{2+} spark expansion [9,10]. In addition, pharmacological activation of VDAC2 with the small molecule efsevin enhances mitochondrial Ca^{2+} uptake, restores cardiac rhythmicity in arrhythmia models, and improves contractile function in failing hearts [11,12]. These observations have positioned VDAC2 as a promising therapeutic target for heart failure and cardiac arrhythmias. Beyond its established role in Ca^{2+} homeostasis, recent evidence has linked VDAC2 to myocardial IRI. Using integrated bioinformatics and experimental validation, a study identified VDAC2 as one of seven key ferroptosis-related genes significantly associated with myocardial IRI, with *in vivo* experiments con-

firming its differential expression in IRI [13]. This finding suggests that VDAC2 may contribute to IRI pathogenesis through mechanisms beyond Ca^{2+} regulation, potentially involving ferroptosis, a novel form of regulated cell death characterized by iron-dependent lipid peroxidation.

Moreover, VDAC2 has been identified as a direct target that suppresses mechanistic target of rapamycin complex 1 (mTORC1) signaling [14]. Interestingly, mTORC1 signaling regulates many metabolic and physiological processes in different tissues and promotes cell growth via activating key anabolic processes, while the dysregulation of mTORC1 causes several diseases, including cancer and diabetes [15,16]. The mTORC1 signaling has also been found to participate in and modulate inflammatory activation, and activated protein C suppresses this signaling via cryoprotective mechanisms in the treatment of IRI [17,18]. Autophagy-related proteins, including mTOR (a key protein in mTORC1 signaling) and Beclin-1, are involved in the treatment of IRI [19]. Besides, Circ_ZNF512-mediated miR-181d-5p inhibition limits cardiomyocyte autophagy and promotes myocardial IRI through an EGR1/mTORC1/TFEB-based mechanism [20]. The downregulation of lysosomal-associated transmembrane protein 4B (LAPTM4B) contributes to myocardial I/R-induced impairment of autophagic flux via modulation of the mTORC1/TFEB pathway [21]. Considering that both ferroptosis and autophagy are implicated in myocardial IRI [22], we speculated that VDAC2 may impact IRI by regulating ferroptosis and apoptosis via the mTORC signaling pathway.

Herein, we explored the role of VDAC2 in regulating H/R-induced ferroptosis of cardiomyocytes through the modulation of mTORC1 signaling, with the aim of providing new insights into the pathogenesis of myocardial IRI.

Materials and Methods

Cell Culture

Rat myocardial cells H9c2 (CRL-1446, American type culture collection, Manassas, VA, USA) were cultured in Dulbecco's Modified Eagle Medium (DMEM) (11965092, Thermo Fisher Scientific, Waltham, MA, USA), supplemented with 10% fetal bovine serum (FBS; 10099141, Thermo Fisher Scientific, Waltham, MA, USA) and 1% Penicillin-Streptomycin Solution (C0222, Beyotime, Shanghai, China). Cells were first thawed in a 37 °C-water bath and then placed in an incubator (ICA175, IRM Technology GmbH, Beijing, China) (37 °C, 5% CO_2). All cell lines were authenticated via short tandem repeat (STR) profiling and simultaneously tested for mycoplasma contamination, with negative results.

Transfection

Small interfering RNA (siRNA) targeting VDAC2 (siVDAC2, siG10831100912-1-5) and its negative control (siNC, siN0000001-1-5) were purchased from RIBOBIO (China) and transfected into H9c2 cells. Lipofectamine™ 2000 Transfection Reagent (11668030, Thermo Fisher Scientific, Waltham, MA, USA) was used for cell transfection. Cells were incubated in a 6-well plate (140675, Thermo Fisher Scientific, Waltham, MA, USA) until reaching 80% confluence. 25 µL diluted siRNA was mixed with 25 µL diluted Lipofectamine® 2000 Reagent in medium at a 1:1 ratio (5 min, room temperature (RT)). The resulting 10 µL siRNA-lipid complex was then added to cells. After 48 h of incubation, cells were harvested for further experiments.

Cell Treatment

First, H9c2 cells were divided into Control and H/R groups. Cells in the H/R group were cultured in glucose-free and FBS-free DMEM (4 h, hypoxia conditions, 5% CO_2, 1% O_2, 94% N_2, 37 °C), and reoxygenated (37 °C, 5% CO_2, 24 h) in DMEM containing 10% FBS [23]. Cells in the control group were cultured under normal conditions at 37 °C with 5% CO_2.

Next, four groups were established, including Control (normal culture), H/R, H/R + siNC, and H/R + siVDAC2. Cells in the last two groups were transfected with siNC and siVDAC2, respectively. Then H9c2 cells in all groups except the Control group experienced hypoxia (4 h) followed by reoxygenation (24 h).

Lastly, H/R, H/R + siNC, H/R + siVDAC2 and H/R + siVDAC2 + Rapamycin (Rap; HY-10219, MedChemExpress, Princeton, NJ, USA) groups were established. Cells in the H/R + siNC and H/R + siVDAC2 groups were transfected with siNC or siVDAC2 and underwent hypoxia and reoxygenation. Cells in the H/R + siVDAC2 + Rap group were transfected with siVDAC2, exposed to hypoxia and reoxygenated, and cultured in DMEM containing 1 µM Rapamycin (the inhibitor of mTORC1 signaling pathway).

Cell Viability

H9c2 cells were seeded in a 96-well plate (163320, Thermo Fisher Scientific, Waltham, MA, USA), after the indicated treatment, cell viability was detected with Cell Counting Kit-8 (CCK-8, HY-K0301, MedChemExpress, Princeton, NJ, USA). 10 µL CCK-8 solution was incubated with cells in a 96-well plate for 1 h. Absorbance at 450 nm was measured using a microplate analyzer (Bk-EL10c, BIOBASE, China).

Western Blotting (WB)

1×10^6 cells were washed with phosphate-buffered saline (PBS; C0221A, Beyotime, Shanghai, China) and lysed in 1 mL of RIPA Lysis Buffer (P0013C, Beyotime, Shanghai, China) containing protease inhibitor cocktail (P1011, Beyotime, Shanghai, China) in EP tubes (3810X, RUNYAO BIOLOGY, Nanjing, China) to extract total protein. Protein concentration was determined using the BCA protein quantitative kit (DQ111-01, TransGen, Beijing,

China). Electrophoretic separation was performed by loading 20 µL protein samples onto SDS-PAGE (NW0412C, Thermo Fisher Scientific, Waltham, MA, USA). Proteins were then transferred onto PVDF membranes (88585, Thermo Fisher Scientific, Waltham, MA, USA), which were blocked with nonfat milk (BI-WB023, Sbjbio, Nanjing, China) and incubated with primary antibodies (16 h, 4 °C). After washing with Tris-Buffered Saline with 0.1% Tween 20 (TBST; ST673, Beyotime, Shanghai, China) on the shaker (thrice, 5 min/time, RT), the membrane was incubated with the secondary antibodies (1 h, RT), and washed with TBST (10 min). The primary and secondary antibodies included VDAC2 (ab126120, 1:500, Abcam, Cambridge, UK), p70s6k (ab186753, 1:1000, Abcam, Cambridge, UK), phosphorylated p70s6k (p-p70s6k) (ab60948, 1:1000, Abcam, Cambridge, UK), Beclin 1 (ab62557, 1:100, Abcam, Cambridge, UK), LC3B (ab192890, 1:2000, Abcam, Cambridge, UK), p-mTOR (#2971, 1:1000, Cell Signaling Technology, Danvers, MA, USA), mTOR (ab32028, 1:1000, Abcam, Cambridge, UK), p-4EBP1 (ab278686, 1:1000, Abcam, Cambridge, UK), 4EBP1 (ab32024, 1:2000, Abcam, Cambridge, UK), β-actin (internal control; ab8226, 1:5000, Abcam, Cambridge, UK), Goat Anti-Rabbit IgG H&L (HRP) (ab6721, 1:10,000, Abcam, Cambridge, UK), Goat Anti-Mouse IgG H&L (HRP) (ab6789, 1:10,000, Abcam, Cambridge, UK). Finally, protein signals were visualized by enhanced chemiluminescence (ECL). In brief, membranes were incubated with mixed ECL substrate (Reagents A:B = 1:1; 17097, Thermo Fisher Scientific, Waltham, MA, USA) and imaged (12012165, Bio-Rad, Hercules, CA, USA).

Quantitative Real-Time PCR (qRT-PCR)

Total RNA was extracted from H9c2 cells with TRIzol™ Reagent (15596-026, Thermo Fisher Scientific, Waltham, MA, USA). Briefly, cells were lysed in 1 mL of TRIzol (2 min), and the homogenate was transferred into 1 mL EP tubes (3810X, RUNYAO BIOLOGY, Nanjing, China), followed by mixing with 200 µL chloroform (151823-50G, Merck, Darmstadt, Germany), shaking for 20 s and centrifugation at 4000 $\times g$ and 4 °C for 15 min (Sorvall Legend MicroCL 17/21, Thermo Fisher Scientific, Waltham, MA, USA). The collected aqueous phase was mixed with 500 µL isopropyl alcohol for 10 min (W292907, Merck, Darmstadt, Germany). After centrifugation (12,000 $\times g$, 10 min, 4 °C), the precipitated RNA was washed with 1 mL of 75% ethanol prepared from 100% ethanol (PHR1373, Merck, Darmstadt, Germany) and DEPC-ddH_2O (SJ01-A, dmdbiomed, Suzhou, China). The RNA precipitate obtained by centrifugation (12,000 $\times g$, 5 min, 4 °C) was dissolved in 30 µL RNase-free H_2O (10977023, Thermo Fisher Scientific, Waltham, MA, USA), followed by RNA concentration measurement with a spectrophotometer (DR6000, HACH, Loveland, CO, USA).

Following reverse transcription of RNA into cDNA (PrimeScript RT Master Mix; RR036A-1, TAKARA, Otsu, Shiga, Japan), the reaction system containing 2 µL 5 × PrimeScript RT Master Mix (Perfect Real Time), total RNA and 10 µL RNase-free ddH_2O were prepared on ice, and incubated together (37 °C, 15 min; 85 °C, 5 s; 4 °C). Then, Real SYBR Mixture (HS0613, HOOSEEN BIOLOGY, Beijing, China) was used. The cDNA template, primers, 2 × SYBR Mixture, and DEPC-ddH_2O were dissolved and placed on ice for subsequent use. A 20 µL reaction mixture was prepared containing 10 µL 2 × SYBR Mixture, 0.5 µL forward primers, 0.5 µL reverse primers, 1 µL cDNA and 8 µL DEPC-ddH_2O. The thermal cycling program was set as follows: initial denaturation at 95 °C for 5 min; 35 cycles of denaturation at 95 °C for 30 s and combined annealing and extension at 60 °C for 1 min. Using the $2^{-\Delta\Delta Ct}$ method, relative mRNA expression levels were calculated [24]. β-actin served as an internal control. Primers used included: VDAC2 sense, 5′-GTGCCATGGTGTGCATGTTT-3′ and antisense, 5′-TGTTTGGGGTTACCAAAGTGA-3′, β-actin sense, 5′-CCTGGCACCCAGCACAAT-3′ and antisense, 5′-GGGCCGGACTCGTCATAC-3′.

Enzyme-Linked Immunosorbent Assay (ELISA)

Rat Creatine Kinase (CK)-MB ELISA Kit (ml059533, mlbio, Shanghai, China) and Rat Lactate dehydrogenase (LDH) ELISA Kit (ml059178, mlbio, Shanghai, China) were used to measure CK and LDH activities in the culture medium supernatant. The standard was diluted 1:1 with sample diluent and added to the reaction wells. Then, 50 µL of standard solution, 50 µL of sample and 50 µL of biotin-labeled antibody were added to each well and co-incubated at 37 °C for 1 h. Wells were then washed with wash solution (30 s, thrice). Subsequently, 80 µL of affinity streptomycin-HRP was added to each sample well and incubated (37 °C, 30 min), followed by three additional washes. Samples were further incubated with 50 µL of substrate A and 50 µL of substrate B at 37 °C for 10 min in the dark, followed by color development (37 °C, 10 min), which was terminated by adding 50 µL of stop buffer. The OD value (450 nm) detection was performed using a spectrophotometer (DR6000, HACH, Loveland, CO, USA).

Iron Content Detection

Ferrous iron (Fe^{2+}) content in H9c2 cells was measured using an Iron Assay Kit (MAK025, Merck, Darmstadt, Germany). First, a 1 mM standard solution was prepared by diluting 10 µL of 100 mM Iron Standard in 990 µL of water. Next, 0, 2, 4, 6, 8 or 10 µL of the 1 mM standard solution was added to 96-well plates to generate 0-10 nmol/well standards, and the volume was adjusted to 100 µL with Iron Assay Buffer, followed by the addition of 5 µL of Iron Reducer to each standard well. 2×10^6 H9c2 cells were then homogenized in 8 volumes of Iron Assay Buffer and then centrifuged (16,000 $\times g$, 4 °C, 10

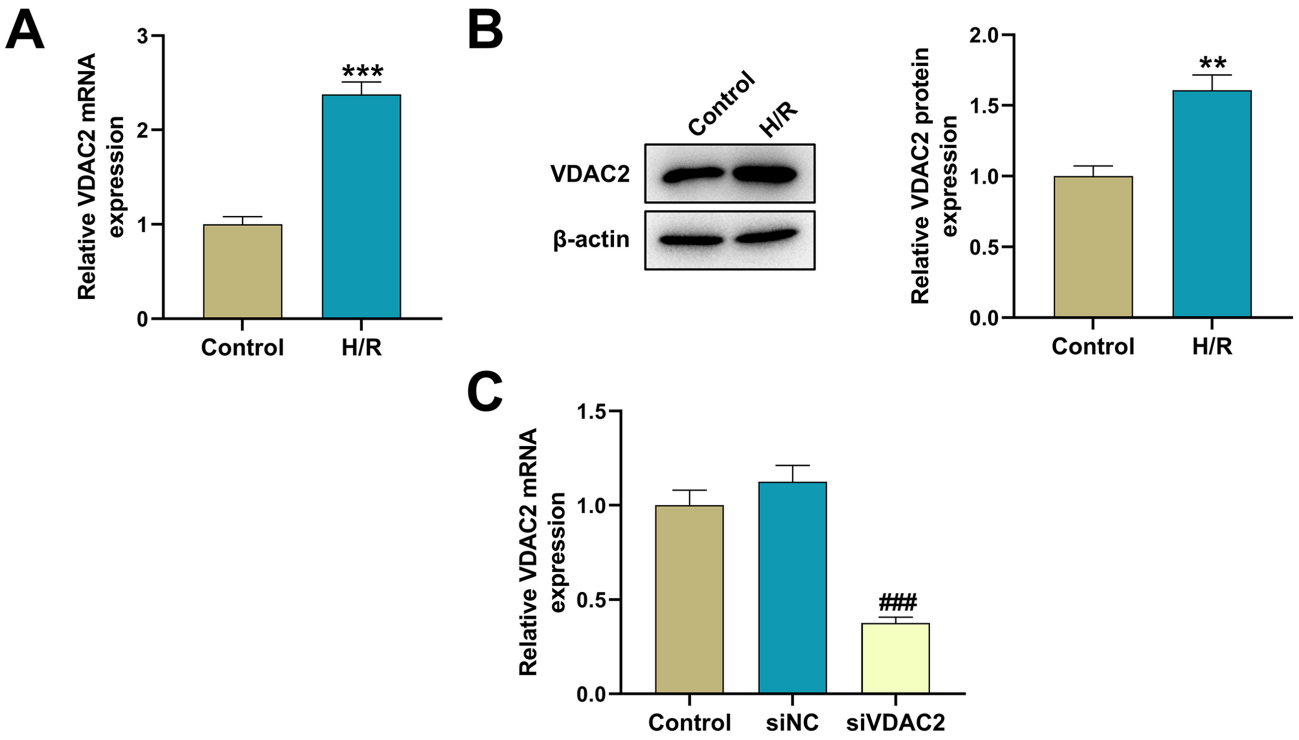

Fig. 1. The expression of VDAC2 was elevated in H/R-induced H9c2 cells. (A,B) VDAC2 expression in H9c2 cells experiencing 4-h hypoxia and 24-h reoxygenation in the H/R group, as shown by qRT-PCR (A) and WB assay (B). An independent samples *t*-test was employed for comparison between two groups. (C) Transfection efficiency in H9c2 cells transfected with siVDAC2 or siNC (qRT-PCR, β-actin as an internal control). One-way ANOVA was used for multi-group comparison, followed by Tukey's post-hoc test. Data are derived from independent experiments (n = 3). $^{**}p < 0.01$, $^{***}p < 0.001$ vs. Control; $^{\#\#\#}p < 0.001$ vs. siNC. VDAC2, voltage-dependent anion channel 2; H/R, hypoxia/reoxygenation; qRT-PCR, Quantitative real-time PCR; WB, Western blotting; siNC, small interfering negative control; ANOVA, analysis of variance.

min). For the sample wells, 20 µL of the supernatant was added, and the volume was adjusted to 100 µL with Iron Assay Buffer, without adding Iron Reducer. After mixing (A mini shaker, E0001, Beyotime, Shanghai, China) and incubation (30 min, 25 °C), 100 µL of Iron Probe was added to each well containing standards and samples. The plate was mixed again and incubated for 60 min at 25 °C (protected from light). Absorbance (593 nm) detection was completed using a spectrophotometer.

Cell Apoptosis Assay

Annexin V-FITC Apoptosis Detection Kit (C1062S, Beyotime, Shanghai, China) was used to measure H9c2 cell apoptosis. Treated H9c2 cells were centrifuged (1000 $\times g$, 10 min) and resuspended in PBS. Then, 5×10^4 cells were centrifuged (1000 $\times g$, 5 min) and suspended in 195 µL of Annexin V-FITC binding buffer. After that, 5 µL of Annexin V-FITC and propidium iodide staining solution were added sequentially. The mixture was incubated (15 min, 25 °C, darkness) and then transferred to an ice bath, followed by apoptosis analysis using a flow cytometer (A24863, Thermo Fisher Scientific, Waltham, MA, USA).

Statistical Analysis

All statistical analyses were conducted using GraphPad Prism 8.0 (GraphPad, San Diego, CA, USA). Measurement data are expressed as mean ± standard deviation. An independent samples *t*-test was employed for comparison between two groups. One-way analysis of variance (ANOVA) was used for multi-group comparison, followed by Tukey's post-hoc test. A p-value < 0.05 was considered statistically significant.

Results

The Expression of VDAC2 Was Improved in H/R-Induced H9c2 Cells

VDAC2 expression in H9c2 cells was quantified using WB and qRT-PCR. Results indicated significantly up-regulated VDAC2 in H9c2 cells in the H/R group (Fig. 1A,B, $p < 0.01$). The data then showed that VDAC2 expression was significantly lower in the siVDAC2 group compared with the siNC group, implying successful transfection (Fig. 1C, $p < 0.001$).

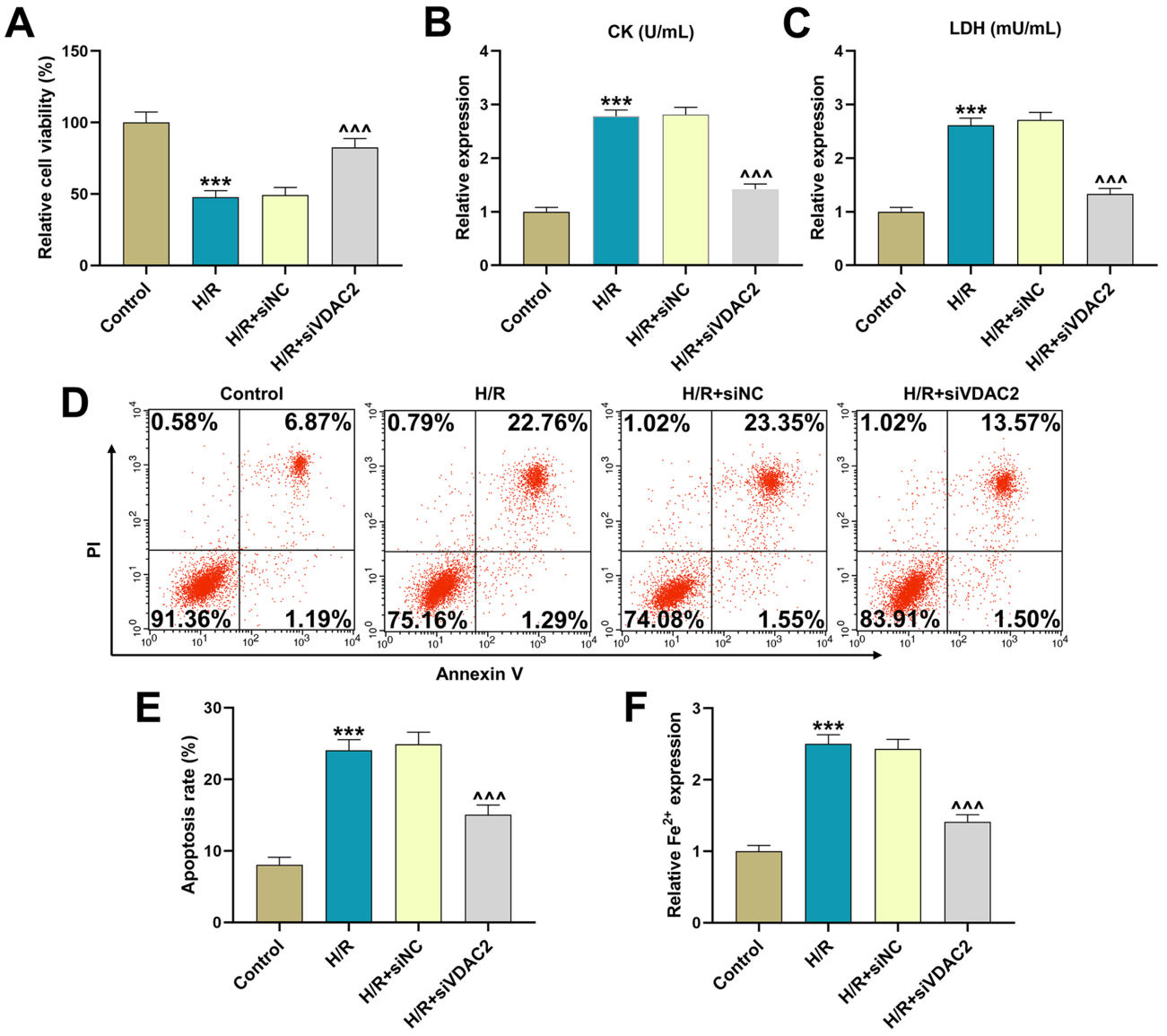

Fig. 2. VDAC2 silencing attenuated the effect of H/R on viability, apoptosis, CK and LDH activities, and Fe^{2+} content in H9c2 cells. (A) The cell viability (Cell counting kit-8) was detected in each group. (B,C) CK and LDH activities in medium supernatant (ELISA) were detected in each group. (D,E) Cell apoptosis (flow cytometer) was detected in each group. (F) Fe^{2+} content (spectrophotometer) was detected in each group. One-way ANOVA was used for multi-group comparison, followed by Tukey's post-hoc test. Data are derived from independent experiments (n = 3). ***$p < 0.001$ vs. Control; $^{\wedge\wedge\wedge}p < 0.001$ vs. H/R + siNC. H/R, hypoxia/reoxygenation; qRT-PCR, Quantitative real-time PCR; WB, Western blotting; CK, Creatine kinase; LDH, Lactate dehydrogenase; ELISA, Enzyme-linked immunosorbent assay; siNC, small interfering negative control.

VDAC2 Silencing Attenuated the Effects of H/R on Viability, Apoptosis, CK and LDH Activities, and Fe^{2+} Content in H9c2 Cells

CCK-8 data revealed that cell viability was notably reduced in the H/R group (Fig. 2A, $p < 0.001$), but higher in the H/R + siVDAC2 group than in the H/R + siNC group (Fig. 2A, $p < 0.001$), denoting that VDAC2 silencing reversed the inhibitory effect of H/R conditions on cell viability. ELISA analysis showed that CK and LDH activities were significantly increased in the H/R group (Fig. 2B,C, $p < 0.001$), and decreased in the H/R + siVDAC2 group (Fig. 2B,C, $p < 0.001$), suggesting that VDAC2 knockdown attenuated the H/R-induced increases in CK and LDH activities in H9c2 cells. Furthermore, H/R stimulation significantly increased H9c2 cell apoptosis (Fig. 2D,E, $p < 0.001$). In contrast to the H/R + siNC group, the H/R + siVDAC2 group displayed reduced H9c2 cell apoptosis (Fig. 2D,E, $p < 0.001$), indicating that VDAC2 knockdown abrogated H/R-induced promotion of cell apoptosis. Fe^{2+} content in H9c2 cells was measured using an Iron Assay Kit and was increased after H/R induction but reduced by siVDAC2 in H/R-induced cells (Fig. 2F, $p < 0.001$).

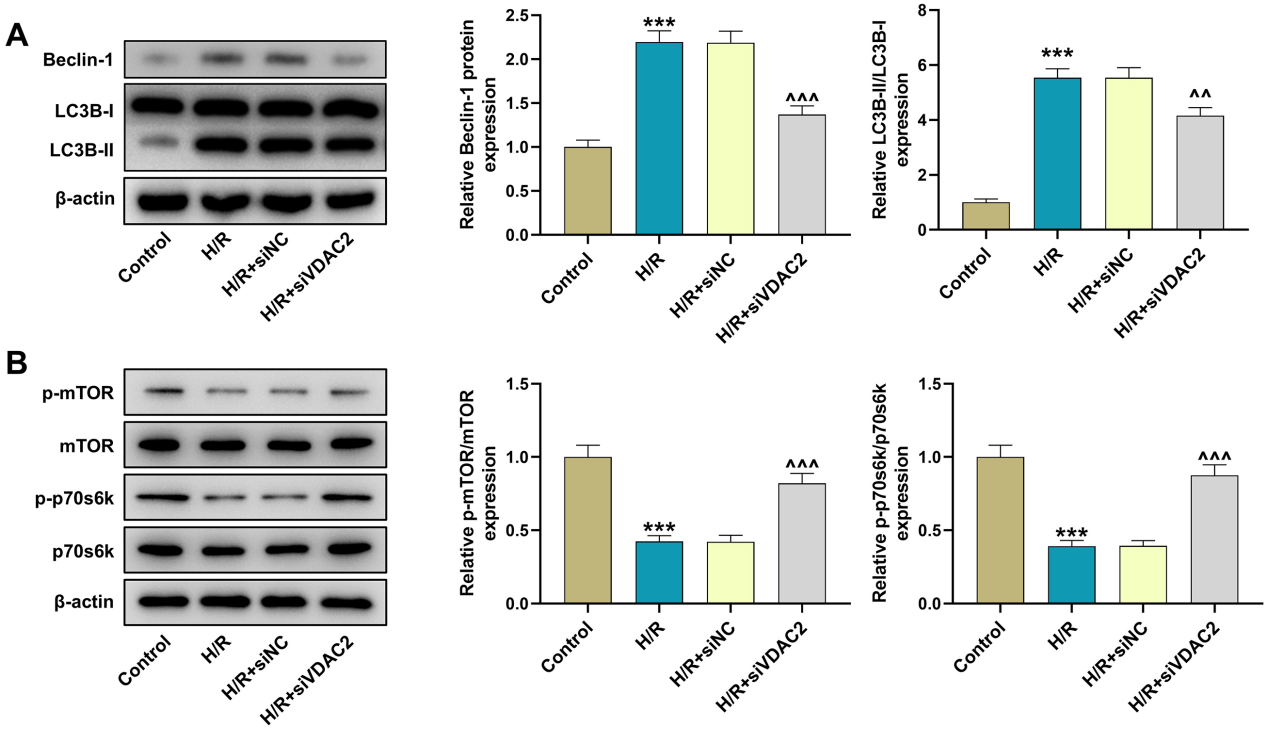

Fig. 3. VDAC2 silencing reversed the effects of H/R on the protein levels related to autophagy and mTORC1 signaling. (A,B) The expression of autophagy/mTOR1 signaling pathway-related proteins (Beclin-1, LC3B-II/LC3B-I, p-mTOR/mTOR, p-p70s6k/p70s6k) (Western Blotting, β-actin as an internal control). One-way ANOVA was used for multi-group comparison, followed by Tukey's post-hoc test. Data are derived from independent experiments (n = 3). ***$p < 0.001$ vs. Control; $^{\wedge\wedge}p < 0.01$, $^{\wedge\wedge\wedge}p < 0.001$ vs. H/R + siNC. H/R, hypoxia/reoxygenation; mTORC1, mechanistic target of rapamycin complex 1.

VDAC2 Silencing Counteracted H/R-Induced Up-Regulation of Beclin-1 and LC3B-II/LC3B-I and Down-Regulation of p-mTOR/mTOR and p-p70s6k/p70s6k

Expression levels of mTORC1 pathway/autophagy-related proteins were assessed using WB. Beclin-1 and LC3B-II/LC3B-I levels were increased by the H/R condition, but the trend was reversed by siVDAC2 (Fig. 3A, $p < 0.01$), manifesting as decreased autophagy. The results further showed down-regulation of p-mTOR/mTOR and p-p70s6k/p70s6k in H/R-induced H9c2 cells (Fig. 3B, $p < 0.001$), which was attenuated by siVDAC2, as evidenced by up-regulation of p-mTOR/mTOR and p-p70s6k/p70s6k (Fig. 3B, $p < 0.001$).

Rap Neutralized the Effects of VDAC2 Silencing on Viability, Apoptosis, Fe^{2+} Content, Autophagy and mTORC1 Signaling in H/R-Induced H9c2 Cells

mTORC1 signaling pathway-related proteins (p-mTOR, mTOR, p-4EBP and 4EBP) were measured using WB. Compared with the H/R + siNC group, the H/R + siVDAC2 group exhibited elevated p-mTOR/mTOR and p-4EBP1/4EBP1 ratios (Fig. 4A, $p < 0.001$). Results also revealed that these two ratios were lower in the H/R + siVDAC2 + Rap group than the H/R + siVDAC2 group (Fig. 4A, $p < 0.001$). Furthermore, VDAC2 silencing activated mTORC1 signaling, an effect that was reversed by Rap. CCK-8 results further revealed that H9c2 cell viability was promoted by siVDAC2 but subsequently suppressed by Rap (Fig. 4B, $p < 0.001$). WB analysis of autophagy-related proteins indicated that Beclin-1 and LC3B-II/LC3B-I levels were reduced in H9c2 cells upon VDAC2 silencing (Fig. 4C, $p < 0.001$); however, Rap intervention restored these autophagic markers (Fig. 4C, $p < 0.05$). H9c2 cell apoptosis was attenuated in the H/R + siVDAC2 group (Fig. 4D,E, $p < 0.001$). In contrast, apoptosis was increased in the H/R + siVDAC2 + Rap group (Fig. 4D,E, $p < 0.01$). Additionally, compared with the H/R + siNC group, the H/R + siVDAC2 group presented decreased levels of Fe^{2+} in H9c2 cells (Fig. 4F, $p < 0.001$), which was subsequently reversed by Rap intervention (Fig. 4F, $p < 0.01$).

Discussion

Myocardial IRI, a consequence of severe impairment of coronary blood supply, contributes to several clinical syndromes [23]. Numerous therapeutic strategies have been explored for the treatment of myocardial IRI. For example, targeting cardiac innervation through peripheral and central nerve stimulation has been proposed as a cardioprotective strategy [25]. Modulating key molecular pathways,

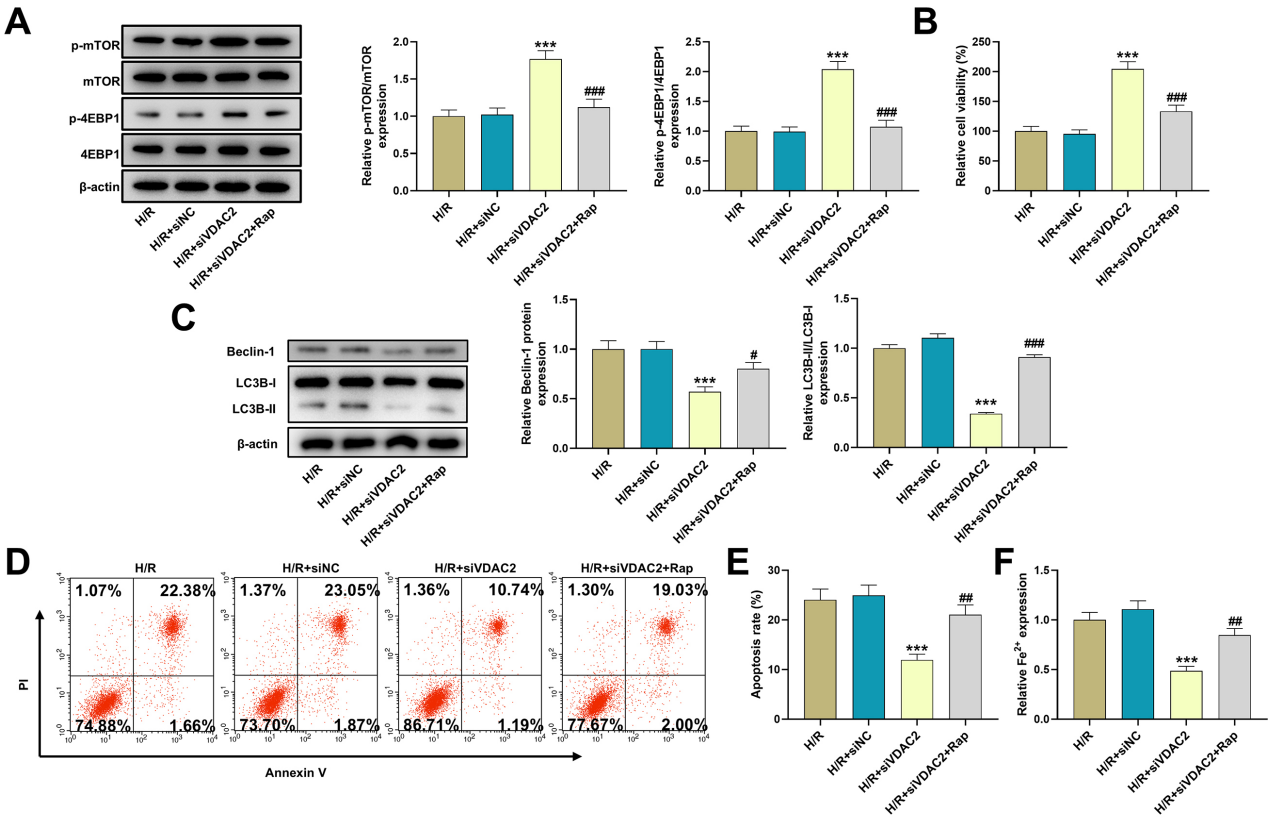

Fig. 4. Rap reversed the effects of VDAC2 silencing on autophagy, mTORC1 signaling, cell apoptosis and Fe^{2+}content. (A) The p-mTOR/mTOR and p-4EBP1/4EBP1 levels (Western Blotting) in different groups. (B) Cell viability (Cell counting kit-8). (C) Autophagy-related proteins (Beclin-1, LC3B-II/-I) (WB). (D,E) Cell apoptosis (Annexin V-FITC Apoptosis Detection Kit). (F) Fe^{2+} content (Iron Assay Kit). β-actin acted as an internal control. One-way ANOVA was used for multi-group comparison, followed by Tukey's post-hoc test. Data are derived from independent experiments (n = 3). $^{***}p < 0.001$ vs. H/R + siNC; $^{\#}p < 0.05$, $^{\#\#}p < 0.01$, $^{\#\#\#}p < 0.001$ vs. H/R + siVDAC2. H/R, hypoxia/reoxygenation; Rap, Rapamycin.

such as STAT and MAPK, has also been proven to effectively mitigate myocardial IRI [26,27].

VDAC2, a mitochondrial porin and VDAC1 isoform, can be used as a hallmark of tumor cell apoptosis and a direct mediator of ceramide-mediated cell death in anticancer treatment [28,29]. Besides, VDAC2 activation by efsevin suppresses arrhythmogenesis, indicating a potential role in antiarrhythmic therapy [30]. Based on existing findings, our study further investigated the underlying mechanism of VDAC2 in myocardial IRI. In our study, VDAC2 expression was elevated in H/R-induced cells, while VDAC2 silencing attenuated cell apoptosis and autophagy, suggesting the involvement of VDAC2 in the progression of myocardial IRI. Accordingly, we further investigated the mechanism of VDAC2 in H/R-induced H9c2 cells.

Moderate IRI preserves cell function and activates recovery systems for survival, while severe IRI induces cell death via apoptotic and necrotic pathways [31]. Moreover, myocardial IRI activates cellular survival programs to regulate reactive oxygen species generation and reduce cell damage. Research has found that apoptosis and autophagy in H9c2 cells can be activated by (Pro)renin receptor through the β-catenin signaling pathway [32]. Besides, myocardial IRI is associated with residual iron following myocardial hemorrhage [33]. VDAC2 can suppress erastin-induced ferroptosis in melanoma, while autophagy activation is necessary for the induction of ferroptosis in normal cells [34]. LC3B-II, LC3B-I and Beclin-1 are autophagy factors, participating in cell proliferation, survival, migration and invasion. Herein, we discovered that VDAC2 silencing inhibited LC3B-II/LC3B-I and Beclin-1 levels in H9c2 cells, indicating that VDAC2 knockdown inhibited autophagy, which in turn suppressed ferroptosis.

The interplay between autophagy and ferroptosis in myocardial IRI has recently emerged as a critical mechanistic axis. It has been reported that STING directly targets glutathione peroxidase 4 (GPX4) to facilitate its autophagic degradation during myocardial I/R injury, thereby promoting ferroptosis [35]. Furthermore, a comprehensive review highlighted that autophagy-dependent ferroptosis plays a central role in myocardial IRI pathogenesis,

with mTOR as a key co-regulatory molecule integrating both pathways [36]. In addition, curcumin attenuates myocardial IRI by inhibiting autophagy-dependent ferroptosis via the Sirt1/AKT/FoxO3a signaling pathway, further supporting the therapeutic potential of targeting this crosstalk [37]. Collectively, these studies establish the autophagy-ferroptosis axis as a central pathogenic mechanism in myocardial IRI [35–38].

According to previous research, VDAC1 functions as a novel upstream regulator of mTOR signaling in endothelial cells, and its overexpression aggravates myocardial IRI under conditions of mTORC2 deficiency [39]. Moreover, VDAC2 and VDAC1 can attenuate the production of Cyclin D1 and inhibit mTORC1 signaling in colon cancer cells [40]. Also, the mTORC1 signaling protects H9c2 cells against myocardial IRI by REDD1 depletion [41]. Herein, VDAC2 silencing activated the mTORC1 signaling pathway and suppressed cell autophagy to mitigate myocardial IRI. To further verify the mechanism of VDAC2 in the mTORC1 signaling pathway, we treated cells with Rap, an inhibitor of mTORC1 [42], and found that Rap reversed the effect of siVDAC2 on myocardial IRI. Rapamycin is a well-established selective inhibitor of mTORC1, and its effective inhibition in cardiomyocyte H/R models has been widely validated [43,44]. Although the inhibitory efficiency of Rapamycin was not independently quantified in this study, its ability to functionally reverse the siVDAC2-induced phenotypes (mTORC1 signaling, autophagy, cell apoptosis and Fe^{2+} content) provides evidence of effective mTORC1 inhibition and supports the conclusion that VDAC2 exerts its protective effects, at least in part, through modulation of mTORC1 signaling.

Conclusion

In conclusion, we demonstrated that VDAC2 deficiency can regulate autophagy and ferroptosis in myocardial IRI cell models. However, our experiment only analyzed the regulatory effect of VDAC2 *in vitro*, and its role *in vivo* has yet to be confirmed. Future studies using animal models will be essential to validate these findings. Collectively, our findings lay the groundwork for future *in vivo* experiments and theoretical exploration of VDAC2.

Availability of Data and Materials

The analyzed datasets generated during the study are available from the corresponding author on reasonable request.

Author Contributions

HJ and YJ designed the research study. CF, BR and JZ performed the research. AY and JF collected and analyzed the data. HJ has been involved in drafting the manuscript and all authors have been involved in revising it critically for important intellectual content. All authors gave final approval of the version to be published. All authors have participated sufficiently in the work to take public responsibility for appropriate portions of the content and agreed to be accountable for all aspects of the work in ensuring that questions related to its accuracy or integrity.

Ethics Approval and Consent to Participate

Not applicable.

Acknowledgment

Not applicable.

Funding

This study was funded by the Tianjin Municipal Health Commission - Key Scientific Research Projects in Traditional Chinese Medicine Field of Tianjin (Grant number 2025018).

Conflict of Interest

The authors declare no conflict of interest.

References

[1] Pastena P, Frye JT, Ho C, Goldschmidt ME, Kalogeropoulos AP. Ischemic cardiomyopathy: epidemiology, pathophysiology, outcomes, and therapeutic options. Heart Failure Reviews. 2024; 29: 287–299. https://doi.org/10.1007/s10741-023-10377-4.

[2] Hao Y, Li R, Fan C, Gao Y, Hou X, Wen W, *et al*. Identification and validation of mitophagy-related genes in acute myocardial infarction and ischemic cardiomyopathy and study of immune mechanisms across different risk groups. Frontiers in Immunology. 2025; 16: 1486961. https://doi.org/10.3389/fimmu.2025.1486961.

[3] Sun X, Lei M, Wang X, Wang J, Li Y, Li C, *et al*. Effect of different diastolic blood pressure levels on the prognosis of patients with heart failure after acute myocardial infarction. Frontiers in Cardiovascular Medicine. 2026; 12: 1703466. https://doi.org/10.3389/fcvm.2025.1703466.

[4] Cui L, Wang Y, Chen W, Huang P, Tang Z, Wang J, *et al*. Coronary microvascular dysfunction and myocardial area at risk assessed by cadmium zinc telluride single photon emission computed tomography after primary percutaneous coronary intervention in acute myocardial infarction patients. Quantitative Imaging in Medicine and Surgery. 2024; 14: 3816–3827. https://doi.org/10.21037/qims-23-1260.

[5] He J, Bellenger NG, Ludman AJ, Shore AC, Strain WD. Treatment of myocardial ischaemia-reperfusion injury in patients with ST-segment elevation myocardial infarction: promise, disappointment, and hope. Reviews in Cardiovascular Medicine. 2022; 23: 23. https://doi.org/10.31083/j.rcm2301023.

[6] Du J, Li Y, Zhao W. Autophagy and Myocardial Ischemia. Advances in Experimental Medicine and Biology. 2020; 1207: 217–222. https://doi.org/10.1007/978-981-15-4272-5_15.

[7] Aljakna Khan A, Sabatasso S. Autophagy in myocardial ischemia and ischemia/reperfusion. Cardiovascular Pathology. 2025; 74: 107691. https://doi.org/10.1016/j.carpath.2024.107691.

[8] Lin D, Cui B, Ma J, Ren J. MiR-183-5p protects rat hearts against myocardial ischemia/reperfusion injury through targeting VDAC1. BioFactors. 2020; 46: 83–93. https://doi.org/10.1002/biof.1571.

[9] Subedi KP, Kim JC, Kang M, Son MJ, Kim YS, Woo SH. Voltage-dependent anion channel 2 modulates resting Ca^{2+} sparks, but not action potential-induced Ca^{2+} signaling in cardiac myocytes. Cell Calcium. 2011; 49: 136–143. https://doi.org/10.1016/j.ceca.2010.12.004.

[10] Zhao K, Zhang Y, Yin Z, Tan L, Juario M, Zhang H, *et al*. GCRV-II major outer capsid protein VP4 promotes cell apoptosis by VDAC2-mediated calcium pathway facilitation. International Journal of Biological Macromolecules. 2025; 285: 138273. https://doi.org/10.1016/j.ijbiomac.2024.138273.

[11] Shimizu H, Schredelseker J, Huang J, Lu K, Naghdi S, Lu F, *et al*. Mitochondrial Ca(2+) uptake by the voltage-dependent anion channel 2 regulates cardiac rhythmicity. eLife. 2015; 4: e04801. https://doi.org/10.7554/eLife.04801.

[12] Schweitzer MK, Wilting F, Sedej S, Dreizehnter L, Dupper NJ, Tian Q, *et al*. Suppression of Arrhythmia by Enhancing Mitochondrial Ca^{2+} Uptake in Catecholaminergic Ventricular Tachycardia Models. JACC. Basic to Translational Science. 2017; 2: 737–747. https://doi.org/10.1016/j.jacbts.2017.06.008.

[13] Zhong C, Dong H, Ma Y, Zhuang B, Shi H, Hong L. Single-cell sequencing combined with transcriptomics and in vivo and in vitro analysis reveals the landscape of ferroptosis in myocardial ischemia-reperfusion injury. FASEB Journal. 2024; 38: e70164. https://doi.org/10.1096/fj.202401056R.

[14] Zhu Z, Zhou X, Du H, Cloer EW, Zhang J, Mei L, *et al*. STING Suppresses Mitochondrial VDAC2 to Govern RCC Growth Independent of Innate Immunity. Advanced Science. 2023; 10: e2203718. https://doi.org/10.1002/advs.202203718.

[15] Shao N, Xi L, Lv Y, Idris M, Zhang L, Cao Y, *et al*. USP5 stabilizes YTHDF1 to control cancer immune surveillance through mTORC1-mediated phosphorylation. Nature Communications. 2025; 16: 1313. https://doi.org/10.1038/s41467-025-56564-9.

[16] Szwed A, Kim E, Jacinto E. Regulation and metabolic functions of mTORC1 and mTORC2. Physiological Reviews. 2021; 101: 1371–1426. https://doi.org/10.1152/physrev.00026.2020.

[17] Duan Q, Yang W, Zhu X, Feng Z, Song J, Xu X, *et al*. Deptor protects against myocardial ischemia-reperfusion injury by regulating the mTOR signaling and autophagy. Cell Death Discovery. 2024; 10: 508. https://doi.org/10.1038/s41420-024-02263-1.

[18] Ren D, Giri H, Li J, Rezaie AR. The Cardioprotective Signaling Activity of Activated Protein C in Heart Failure and Ischemic Heart Diseases. International Journal of Molecular Sciences. 2019; 20: 1762. https://doi.org/10.3390/ijms20071762.

[19] Shi B, Ma M, Zheng Y, Pan Y, Lin X. mTOR and Beclin1: Two key autophagy-related molecules and their roles in myocardial ischemia/reperfusion injury. Journal of Cellular Physiology. 2019; 234: 12562–12568. https://doi.org/10.1002/jcp.28125.

[20] Huang C, Shu L, Zhang H, Zhu X, Huang G, Xu J. Circ_ZNF512-Mediated miR-181d-5p Inhibition Limits Cardiomyocyte Autophagy and Promotes Myocardial Ischemia/Reperfusion Injury through an EGR1/mTORC1/TFEB-Based Mechanism. Journal of Medicinal Chemistry. 2022; 65: 1808–1821. https://doi.org/10.1021/acs.jmedchem.1c00745.

[21] Gu S, Tan J, Li Q, Liu S, Ma J, Zheng Y, *et al*. Downregulation of LAPTM4B Contributes to the Impairment of the Autophagic Flux via Unopposed Activation of mTORC1 Signaling During Myocardial Ischemia/Reperfusion Injury. Circulation Research. 2020; 127: e148–e165. https://doi.org/10.1161/CIRCRESAHA.119.316388.

[22] Wei YL, Cheng L, Chen XY, Qiao Q, Ye XR, Wang D, *et al*. Ferroptosis in ischemia-reperfusion injury: molecular mechanisms and therapeutic strategies. American Journal of Cardiovascular Disease. 2025; 15: 405–441. https://doi.org/10.62347/OLGV6926.

[23] Qiu L, Xu C, Xia H, Chen J, Liu H, Jiang H. Downregulation of P300/CBP-Associated Factor Attenuates Myocardial Ischemia-Reperfusion Injury Via Inhibiting Autophagy. International Journal of Medical Sciences. 2020; 17: 1196–1206. https://doi.org/10.7150/ijms.44604.

[24] Livak KJ, Schmittgen TD. Analysis of relative gene expression data using real-time quantitative PCR and the 2(–Delta Delta C(T)) Method. Methods. 2001; 25: 402–408. https://doi.org/10.1006/meth.2001.1262.

[25] Omoto ACM, do Carmo JM, Nelson B, Aitken N, Dai X, Moak S, *et al*. Central Nervous System Actions of Leptin Improve Cardiac Function After Ischemia-Reperfusion: Roles of Sympathetic Innervation and Sex Differences. Journal of the American Heart Association. 2022; 11: e027081. https://doi.org/10.1161/JAHA.122.027081.

[26] Chen W, Zhang Y, Wang Z, Tan M, Lin J, Qian X, *et al*. Dapagliflozin alleviates myocardial ischemia/reperfusion injury by reducing ferroptosis *via* MAPK signaling inhibition. Frontiers in Pharmacology. 2023; 14: 1078205. https://doi.org/10.3389/fphar.2023.1078205.

[27] Xu M, Li X, Song L. Baicalin regulates macrophages polarization and alleviates myocardial ischaemia/reperfusion injury via inhibiting JAK/STAT pathway. Pharmaceutical Biology. 2020; 58: 655–663. https://doi.org/10.1080/13880209.2020.1779318.

[28] Dadsena S, Bockelmann S, Mina JGM, Hassan DG, Korneev S, Razzera G, *et al*. Ceramides bind VDAC2 to trigger mitochondrial apoptosis. Nature Communications. 2019; 10: 1832. https://doi.org/10.1038/s41467-019-09654-4.

[29] Patel SJ, Chen ZJ. VDAC2 brake release: unleashing inflammation via IFNγ. Trends in Pharmacological Sciences. 2025; 46: 695–696. https://doi.org/10.1016/j.tips.2025.07.001.

[30] Wilting F, Kopp R, Gurnev PA, Schedel A, Dupper NJ, Kwon O, *et al*. The antiarrhythmic compound efsevin directly modulates voltage-dependent anion channel 2 by binding to its inner wall and enhancing mitochondrial Ca^{2+} uptake. British Journal of Pharmacology. 2020; 177: 2947–2958. https://doi.org/10.1111/bph.15022.

[31] Liu Y, Li L, Wang Z, Zhang J, Zhou Z. Myocardial ischemia-reperfusion injury; Molecular mechanisms and prevention. Microvascular Research. 2023; 149: 104565. https://doi.org/10.1016/j.mvr.2023.104565.

[32] Gao X, Zhang S, Wang D, Cheng Y, Jiang Y, Liu Y. (Pro)renin receptor contributes to hypoxia/reoxygenation-induced apoptosis and autophagy in myocardial cells via the beta-catenin signaling pathway. Physiological Research. 2020; 69: 427–438. https://doi.org/10.33549/physiolres.934210.

[33] Zhou D, Yang Y, Han R, He J, Liu D, Xia W, *et al*. Ferroptosis and its Potential Determinant Role in Myocardial Susceptibility to Ischemia/Reperfusion Injury in Diabetes. Reviews in Cardiovascular Medicine. 2024; 25: 360. https://doi.org/10.31083/j.rcm2510360.

[34] Yang Y, Luo M, Zhang K, Zhang J, Gao T, Connell DO, *et al*. Nedd4 ubiquitylates VDAC2/3 to suppress erastin-induced ferroptosis in melanoma. Nature Communications. 2020; 11: 433. https://doi.org/10.1038/s41467-020-14324-x.

[35] Wang X, Chen T, Chen S, Zhang J, Cai L, Liu C, *et al*. STING aggravates ferroptosis-dependent myocardial ischemia-reperfusion injury by targeting GPX4 for autophagic degradation. Signal Transduction and Targeted Therapy. 2025; 10: 136. https://doi.org/10.1038/s41392-025-02216-9.

[36] Yang X, Wu H, Liu D, Zhou G, Zhang D, Yang Q, *et al*. The link between ferroptosis and autophagy in myocardial ischemia/reperfusion injury: new directions for therapy. Journal

of Cardiovascular Translational Research. 2025; 18: 408–423. https://doi.org/10.1007/s12265-025-10590-6.

[37] Zhao ST, Qiu ZC, Xu ZQ, Tao ED, Qiu RB, Peng HZ, *et al*. Curcumin attenuates myocardial ischemia-reperfusion-induced autophagy-dependent ferroptosis via Sirt1/AKT/FoxO3a signaling. International Journal of Molecular Medicine. 2025; 55: 51. https://doi.org/10.3892/ijmm.2025.5492.

[38] Liu J, Kuang F, Kroemer G, Klionsky DJ, Kang R, Tang D. Autophagy-Dependent Ferroptosis: Machinery and Regulation. Cell Chemical Biology. 2020; 27: 420–435. https://doi.org/10.1016/j.chembiol.2020.02.005.

[39] Head SA, Shi W, Zhao L, Gorshkov K, Pasunooti K, Chen Y, *et al*. Antifungal drug itraconazole targets VDAC1 to modulate the AMPK/mTOR signaling axis in endothelial cells. Proceedings of the National Academy of Sciences of the United States of America. 2015; 112: E7276–E7285. https://doi.org/10.1073/pnas.1512867112.

[40] Aono Y, Horinaka M, Iizumi Y, Watanabe M, Taniguchi T, Yasuda S, *et al*. Sulindac sulfone inhibits the mTORC1 pathway in colon cancer cells by directly targeting voltage-dependent anion channel 1 and 2. Biochemical and Biophysical Research Communications. 2018; 505: 1203–1210. https://doi.org/10.1016/j.bbrc.2018.10.050.

[41] Li P, Lin N, Guo M, Huang H, Yu T, Zhang L. REDD1 knockdown protects H9c2 cells against myocardial ischemia/reperfusion injury through Akt/mTORC1/Nrf2 pathway-ameliorated oxidative stress: An in vitro study. Biochemical and Biophysical Research Communications. 2019; 519: 179–185. https://doi.org/10.1016/j.bbrc.2019.08.095.

[42] Wang Z, Huang Y, Zhang Y, Zhu H, Amin MR, Chen R, *et al*. Knockdown of SESN2 Exacerbates Cerebral Ischemia-Reperfusion Injury Through Enhancing Glycolysis via the mTOR/HIF-1α Pathway. CNS Neuroscience & Therapeutics. 2025; 31: e70314. https://doi.org/10.1111/cns.70314.

[43] Chen B, Fan P, Song X, Duan M. The role and possible mechanism of the ferroptosis-related SLC7A11/GSH/GPX4 pathway in myocardial ischemia-reperfusion injury. BMC Cardiovascular Disorders. 2024; 24: 531. https://doi.org/10.1186/s12872-024-04220-3.

[44] Yang K, Kong X, Xie C, Chen Y, Zou Z, Wang X, *et al*. Combined administration of dexmedetomidine and propofol mitigates myocardial ischemia/reperfusion injury by modulating the Akt/mTOR/Nrf2 axis to suppress ferroptosis. European Journal of Pharmacology. 2025; 997: 177599. https://doi.org/10.1016/j.ejphar.2025.177599.